

# $P - V$ criticality and geometrothermodynamics of black holes with Born-Infeld type nonlinear electrodynamics

S. H. Hendi<sup>1,2\*</sup>, S. Panahiyan<sup>1†</sup> and B. Eslam Panah<sup>1‡</sup>

<sup>1</sup> *Physics Department and Biruni Observatory, College of Sciences, Shiraz University, Shiraz 71454, Iran*

<sup>2</sup> *Research Institute for Astronomy and Astrophysics of Maragha (RIAAM), Maragha, Iran*

In this paper, we take into account the black hole solutions of Einstein gravity in the presence of logarithmic and exponential forms of nonlinear electrodynamics. At first, we consider the cosmological constant as a dynamical pressure to study the analogy of the black hole solutions with the Van der Waals liquid–gas system in the extended phase space. We plot  $P - v$ ,  $T - v$  and  $G - T$  diagrams and investigate the phase transition of adS black holes in the canonical ensemble. We study the nonlinearity effects of electrodynamics and see how the power of nonlinearity affects critical behavior and phase transition of the system. We also investigate the effects of dimensionality on the critical values and analyze its crucial role. Moreover, we show the changes in the universal ratio  $P_c v_c / T_c$  for variation of different parameters. In addition, we make a comparison between linear and nonlinear electromagnetic fields and show that the lowest critical temperature belongs to Maxwell theory. Also, we make some arguments regarding to how power of nonlinearity brings the system to Schwarzschild–like and Reissner–Nordström–like limitations. Next, we study the critical behavior of the system in context of heat capacity. We show that critical behavior of system is similar to the one in phase diagrams of extended phase space. We point out that phase transition points of the extended phase space only appear as divergencies of heat capacity. We also extend the study of phase transition points through geometrothermodynamics (GTD) method. We introduce two new thermodynamical metrics for extended phase space and show that divergencies of thermodynamical Ricci scalar of the new metrics coincide with phase transition points of the system. The characteristic behavior of these divergencies, hence critical points is exactly the one that is obtained in extended phase space and heat capacity. Then, we introduce a new method for obtaining critical pressure and horizon radius by considering denominator of the heat capacity. We show that there are several benefits that make this approach favorable comparing to other ones.

## I. INTRODUCTION

In recent years, there has been an increasing interest in asymptotically anti-de Sitter black holes. This is mainly based on the fact that there is an equivalence of string theory on asymptotically anti de-Sitter spacetimes and the quantum field theory living on the boundary of them [1–4]. Although Einstein had inserted the cosmological constant as a fixed parameter in the gravitational field equations, in an increasing number of recent papers it was shown that it might be regarded as a variable [5, 6]. In other words, following the recent idea of including the cosmological constant in the first law of black hole thermodynamics, the cosmological constant is no longer a fixed parameter, but rather a thermodynamical variable.

Regarding the extended phase space of black holes thermodynamics, one may treat the cosmological constant as a dynamical pressure [7–17]. The results are much richer thermodynamics than heretofore, and interestingly, it is shown that the critical behavior of black holes is analogous to the Van der Waals liquid–gas phase transition. So, investigation of the mentioned extending phase space and its phase transition have gained a lot of attention recently [7–17]. Thermodynamic properties and phase transition of the asymptotically anti de-Sitter black holes was studied by Hawking and Page [18]. Witten [19] reconsidered the Hawking–Page phase transition in the context of gauge theory and AdS/CFT correspondence. Generally we should note that phase transition plays an important role in describing different phenomena in thermodynamics and quantum point of views.

On the other side, although Maxwell theory is capable of describing different phenomena in electrodynamics domain, it fails regarding some important issues (for various limitations of the Maxwell theory see Ref. [20, 21] for more details). In order to solve these problems, one may regard the nonlinear electrodynamics [22–31]. In recent years, investigation of nonlinear electrodynamics has got a new impetus. Strong motivation comes from developments in string/M-theory, which is a promising approach to quantum gravity [32]. It has been shown that the Born-Infeld [33] (BI) type theories are specific in the context of NLED models and naturally arise in the low-energy limit of heterotic string theory

---

\* email address: hendi@shirazu.ac.ir

† email address: zixify@gmail.com

‡ email address: behzad\_eslampanah@yahoo.com

[34–39]. In recent years, other BI types of NLED have been introduced, in which can remove the divergency of the electric field of point charge near the origin. The Lagrangians of logarithmic and exponential forms of NLED theories were, respectively, proposed by Soleng [30] and Hendi [31] with the following explicit forms

$$\mathcal{L}(\mathcal{F}) = \begin{cases} \beta^2 \left( \exp\left(-\frac{\mathcal{F}}{\beta^2}\right) - 1 \right), & ENEF \\ -8\beta^2 \ln\left(1 + \frac{\mathcal{F}}{8\beta^2}\right), & LNEF \end{cases}. \quad (1)$$

where  $\beta$  is nonlinearity parameter.

In this paper, we consider asymptotically anti-de Sitter black hole solutions of the Einstein gravity in the presence of the recent BI type NLED to investigate the extended phase space thermodynamics and  $P - v$  criticality of the solutions and also phase transition points through GTD.

Thermodynamical geometry is another approach for studying phase transition of black holes. It means that, by studying the divergence points of thermodynamical Ricci scalar (TRS), we can investigate phase transition points for black holes. In other words, it is expected that divergencies of TRS coincide with phase transition points of the black holes. In 1975 Weinhold [40] introduced differential geometric concepts into ordinary thermodynamics by considering a kind of metric defined as the second derivatives of internal energy with respect to entropy and other extensive quantities for a thermodynamical system. After that, Ruppeiner [41] introduced another metric and defined the minus second derivatives of entropy with respect to the internal energy and other extensive quantities. It is notable that, the Ruppeiner metric is conformal to the Weinhold metric with the inverse temperature as the conformal factor. Both thermodynamical metrics have been applied to study the thermodynamical geometry of ordinary systems [42–45]. In particular, it was found that the Ruppeiner geometry carries information regarding phase structure of thermodynamical systems. Because of their success for their applications in ordinary thermodynamical systems, they have also been employed to study black hole phase structures which led to interesting results [46–50].

Since these two approaches fail in order to describe phase transition of several black holes [51], Quevedo proposed new types of thermodynamical metrics for studying geometrical structure of the black hole thermodynamics [52, 53]. This method was employed to study the geometrical structure of the phase transition of black holes [54–59] and proved to be a strong machinery for describing phase transition of black holes. However, this approach was not without any problem [51]. Hence for eliminating the problems of previous thermodynamical metrics, Hendi et al. proposed a new metric in Ref. [51].

Let us begin with the following  $d$ -dimensional spherically symmetric line element

$$ds^2 = -g(r)dt^2 + \frac{dr^2}{g(r)} + r^2 d\Omega_{d-2}^2, \quad (2)$$

where  $d\Omega_d^2$  denotes the standard metric of  $d$ -dimensional sphere  $S^d$  with the volume  $\omega_d$ . In what follows, we consider Einstein gravity coupled with the mentioned BI type NLED models [59–62]. It was shown that, regardless of gravitational sector, one may use the following electromagnetic field equation to obtain related gauge potential

$$\nabla_\mu \left( \frac{d\mathcal{L}(\mathcal{F})}{d\mathcal{F}} F^{\mu\nu} \right) = 0, \quad (3)$$

in which the nonzero component of gauge potential is  $A_t$  [59, 60]

$$A_t = \begin{cases} \frac{\beta r \sqrt{L_W}}{2(d-3)(3d-7)} [3d-7 + (d-2)\varpi L_W], & ENEF \\ \frac{2\beta^2 r^{d-1}}{q(d-1)} [1 - \varpi'], & LNEF \end{cases}, \quad (4)$$

where

$$\begin{aligned} \varpi &= {}_1F_1 \left( [1], \left[ \frac{5d-11}{2d-4} \right], \frac{L_W}{2d-4} \right), \\ \varpi' &= {}_2F_1 \left( \left[ \frac{-1}{2}, \frac{1-d}{2d-4} \right], \left[ \frac{d-3}{2d-4} \right], 1 - \Gamma^2 \right), \end{aligned}$$

and the Lambert function  $L_W = \text{LambertW} \left( \frac{4q^2}{\beta^2 r^{2d-4}} \right)$ ,  $\Gamma = \sqrt{1 + \frac{q^2}{\beta^2 r^{2d-4}}}$  and  $q$  is an integration constant related to the the total electric charge  $Q = \frac{V_{d-2}}{8\pi} q$ . The electric potential  $U$ , measured at infinity with respect to the event horizon, is  $U = -A_t$ . It is easy to show that the electric field may be written as [59, 60]

$$E(r) = F_{tr} = \frac{Q}{r^2} \times \begin{cases} e^{-\frac{L_W}{2}}, & ENEF \\ \frac{2}{\Gamma+1}, & LNEF \end{cases}. \quad (5)$$

## II. EXTENDED PHASE SPACE AND $P - V$ CRITICALITY IN EINSTEIN GRAVITY

Starting with the Einstein gravity in the presence of NLED, we consider the following field equation

$$G_{\mu\nu} + \Lambda g_{\mu\nu} = \frac{1}{2}g_{\mu\nu}\mathcal{L}(\mathcal{F}) - 2\frac{d\mathcal{L}(\mathcal{F})}{d\mathcal{F}}F_{\mu\lambda}F_{\nu}^{\lambda}, \quad (6)$$

with the following solutions for the metric function [59, 60]

$$g(r) = 1 - \frac{2\Lambda r^2}{(d-1)(d-2)} - \frac{m}{r^{d-3}} - \frac{8\beta^2 r^2 \Upsilon}{(d-1)(d-2)}, \quad (7)$$

$$\Upsilon = \begin{cases} 1 + \frac{2(d-1)q}{\beta r^{d-1}} \left[ \int \left( \sqrt{L_W} - \frac{1}{\sqrt{L_W}} \right) dr \right], & ENEF \\ \frac{(2d-3)(\Gamma-1)}{(d-1)} - \ln\left(\frac{1+\Gamma}{2}\right) + \mathcal{H}, & LNEF \end{cases},$$

$$\mathcal{H} = \frac{(d-2)^2 (1-\Gamma^2) {}_2F_1\left(\left[\frac{1}{2}, \frac{d-3}{2d-4}\right], \left[\frac{3d-7}{2d-4}\right], 1-\Gamma^2\right)}{(d-1)(d-3)},$$

where  $m$  is an integration constant which is related to the total mass. Looking for the curvature singularity of the metric (2), one finds that the Kretschmann scalar diverges at  $r = 0$ . In addition, numerical analysis shows that the metric functions have at least one real positive root. Moreover, using series expansion of metric function for large values of  $r$ , we find that the dominant term is related to  $\Lambda$ . Consequently, we deduce that these solutions may be interpreted as asymptotically anti de-Sitter black holes.

Now, we take into account the surface gravity interpretation to obtain the Hawking temperature of the mentioned black hole solutions

$$T = \frac{-2\Lambda r_+^2 + (d-2)(d-3) - \Phi}{4\pi r_+ (d-2)}, \quad (8)$$

$$\Phi = \begin{cases} \beta^2 r_+^2 \left( \left[ 1 + \left( \frac{2E}{\beta} \right)^2 \right] e^{-\frac{2E^2}{\beta^2}} - 1 \right), & ENEF \\ 8r_+^2 \beta^2 \ln \left[ 1 - \left( \frac{E}{2\beta} \right)^2 \right] + \frac{4r_+^2 E^2}{1 - \left( \frac{E}{2\beta} \right)^2}, & LNEF \end{cases}$$

The finite mass of black hole can be obtained by using the behavior of the metric at large distances [63]

$$M = \frac{\omega_{d-2} (d-2) m}{16\pi}, \quad (9)$$

where one may obtain the parameter  $m$  from the fact that the metric functions vanish at the event horizon,  $r_+$ . The black hole entropy of Einstein gravity may be determined from the area law

$$S = \frac{\omega_{d-2}}{4} r_+^{d-2}. \quad (10)$$

Here, we regard  $\Lambda$  as a thermodynamical pressure  $P = \frac{-\Lambda}{8\pi}$  and its corresponding conjugate quantity is the thermodynamical volume which one can obtain with following relation

$$V = \left( \frac{\partial H}{\partial P} \right)_{S,Q}. \quad (11)$$

Due to fact that we are considering cosmological constant as thermodynamical pressure, the interpretation of mass will be different from previous one. Usually mass of the black hole is interpreted as internal energy. But by considering such relation between cosmological constant and thermodynamical pressure, the interpretation of mass will become enthalpy. In other words, mass of the black hole has more contribution to thermodynamical construction of the system. As a result of this new insight regarding mass, Gibbs free energy of the system will be given by

$$G = H - TS = M - TS \quad (12)$$

Now, we would like to study the phase transition of Einstein black hole solutions in canonical ensemble with the mentioned NLED models. Using Eq. (8), one can obtain the following equation of state

$$P = \frac{(d-2)T}{4r_+} - \frac{(d-2)(d-3) - \Phi}{16\pi r_+^2}, \quad (13)$$

where  $r_+$  is linear function of the specific volume  $v$  in geometric unit [7–17]. In general, for these thermodynamical systems, we have the following result for volume

$$V = \left( \frac{\partial M}{\partial P} \right)_{S,Q} = \frac{\omega_{d-2} r_+^{d-1}}{d-1}, \quad (14)$$

which is in agreement with the topological structure of our spacetime (spherical symmetric). This approval is a confirmation for considering cosmological constant as a thermodynamical pressure.

Besides, we know that the Smarr formula may be extended to nonlinear theories of electrodynamics [64–67]. In order to obtain an extension of the first law and its related modified Smarr formula, one can use geometrical techniques (scaling argument). Here,  $M$  should be the function of entropy, pressure, charge and BI parameter [64–67]. Regarding obtained quantities, we find that they satisfy the following differential form

$$dM = TdS + \Phi dQ + VdP + \mathcal{B}d\beta. \quad (15)$$

where we have calculated  $T$  and  $\Phi$ , and one can obtain

$$V = \left( \frac{\partial M}{\partial P} \right)_{S,Q,\beta},$$

$$\mathcal{B} = \left( \frac{\partial M}{\partial \beta} \right)_{S,Q,P}.$$

In addition, taking into account the scaling argument, we can obtain the generalized Smarr relation (per unit volume  $\omega_{d-2}$ ) for our asymptotically adS solutions in the extended phase space

$$(d-3)M = (d-2)TS + (d-3)Q\Phi - 2PV - \mathcal{B}\beta \quad (16)$$

where

$$V = \frac{r_+^{d-1}}{d-1},$$

$$\mathcal{B}|_{\text{ENED}} = \frac{q(d-2)r_+ F\left([1], \left[\frac{5d-11}{2d-4}\right], \frac{L_{W+}}{2d-4}\right)}{8\pi(d-1)(3d-7)(L_{W+})^{\frac{-3}{2}}} - \frac{\beta r_+^{d-1}}{8\pi(d-1)} + \frac{q\beta r_+^d \sqrt{L_{W+}}(1-L_{W+})}{8\pi(d-1)(1+L_{W+})} + \frac{2qr_+(1+L_{W+})^{-1}}{8\pi(d-1)\sqrt{L_{W+}}},$$

$$\mathcal{B}|_{\text{LNED}} = \frac{\beta r_+^{d-1}}{2\pi} \left[ \frac{(d-2)(\Gamma_+^2 - 1)}{(d-1)^2} F\left(\left[\frac{1}{2}, \frac{d-3}{2d-4}\right], \left[\frac{3d-7}{2d-4}\right], 1 - \Gamma_+^2\right) + \frac{2\ln\left(\frac{1+\Gamma_+}{2}\right)}{(d-1)} + \frac{(3d-5)(1-\Gamma_+)}{(d-1)^2} \right].$$

The next step will be devoted to obtain critical values. In order to investigate phase transition and the behavior of these thermodynamical systems, we work in geometric unit and draw graphs of  $P - v$ ,  $T - v$  and  $G - T$  diagrams.

Now, we are in a position to analyze the plot of  $P - v$  isotherm diagram and investigate the existence of phase transition. In general, LNEF and ENEF models for large value of nonlinearity parameter have similar asymptotical behavior. Moreover, thermodynamical behavior of black hole solutions with the mentioned models are the same, globally. Therefore, for economical reason, we will plot phase diagrams for LNEF case. Left diagrams of Figs. 1 - 5 indicates an analogue behavior between our plots with those of Van der Waals gas. One may use the inflection point properties of critical point to obtain

$$\left( \frac{\partial P}{\partial v} \right)_T = 0, \quad (17)$$

$$\left( \frac{\partial^2 P}{\partial v^2} \right)_T = 0. \quad (18)$$

These equations help us to obtain the critical values for the temperature, the pressure and the volume. Although we cannot, analytically, obtain the critical values of the temperature, volume and pressures, we may investigate them numerically. Taking into account the critical quantities, one can obtain the following universal ratio

$$\rho_c = \frac{P_c v_c}{T_c}. \quad (19)$$

Besides, one may look for the phase transition with the help of  $T - v$  diagrams. These graphs are also representing phase transition of black holes which is of an interest in this paper. Also, with drawing these figures one can see whether the obtained critical values are essentially critical values representing phase transition. Another reason for studying  $T - v$  diagrams is due to the fact that comparing to other graphs ( $P - v$  and  $G - T$ ), that are used for studying critical behavior of the system,  $T - v$  plots give us better insight in understanding single phase regions and the effects of different parameters on these single phase regions. In our case, these single phase regions are representing small/large (unstable/stable) black holes. On the other hand, if one is interested in superconductivity that these nonlinear theories represent, studying of these diagrams gives better description regarding conductor/superconductor regions and what modifies them. We plot the mentioned figures in the middle diagram of Figs. 1 - 5. These plots indicate an inflection point which shows the phase transition of the system. Moreover, phase transition of a thermodynamical system can be studied by Gibbs free energy. We follow the method of the extended phase space to obtain Gibbs free energy. The behavior of the Gibbs free energy with respect to the temperature is displayed in right diagrams of Figs. 1 - 5. In these figures the characteristic swallow-tail behavior guarantees the existence of the phase transition.

Table (1):  $q = 1, d = 5.$

| $\beta$ | $v_c$  | $T_c$  | $P_c$  | $\frac{P_c v_c}{T_c}$ |
|---------|--------|--------|--------|-----------------------|
| 0.1000  | 0.4012 | 0.4004 | 0.2449 | 0.2454                |
| 0.5000  | 1.4142 | 0.1744 | 0.0375 | 0.3044                |
| 1.0000  | 1.4765 | 0.1712 | 0.0360 | 0.3106                |
| 1.5000  | 1.4870 | 0.1707 | 0.0357 | 0.3117                |
| 2.0000  | 1.4907 | 0.1705 | 0.0356 | 0.3120                |

Table (2):  $q = 1, d = 7.$

| $\beta$ | $v_c$  | $T_c$  | $P_c$  | $\frac{P_c v_c}{T_c}$ |
|---------|--------|--------|--------|-----------------------|
| 0.1000  | 0.7380 | 0.6526 | 0.4410 | 0.4987                |
| 0.5000  | 1.1549 | 0.4769 | 0.2264 | 0.5483                |
| 1.0000  | 1.1944 | 0.4711 | 0.2207 | 0.5597                |
| 1.5000  | 1.2014 | 0.4698 | 0.2195 | 0.5612                |
| 2.0000  | 1.2037 | 0.4694 | 0.2191 | 0.5618                |

### III. DISCUSSION ON THE RESULTS OF DIAGRAMS

As one can see, thermodynamical behavior of our systems is presented in Figs. 1 - 5. The obtained critical values are representing a phase transition point which is evident from swallowtail appearing in  $G - T$  diagrams. On the other hand, studying  $P - v$  and  $T - v$  graphs for related critical values shows that obtained values are critical point that phase transition occurs in them. As nonlinearity parameter increases, the temperature, in which phase transitions take place, decreases and the value of Gibbs free energy of phase transition points increases. These results indicate that in more powerful nonlinearity parameter our thermodynamical system needs less energy in order to have a phase transition (see the middle and right diagrams of Fig. 4 for more details). This could also be interpreted from the fact that as nonlinearity parameter increases, the Enthalpy which is represented by total finite mass of black hole increases, too. Therefore, for obtained black holes we expect to phase transition occurs with absorbing less mass form surrounding.

Studying  $P - v$  diagram shows that as  $\beta$  increases, the critical pressure decreases, but in opposite side the horizon radius of critical points increases. Also, one can see that as the nonlinearity parameter increases the distance between

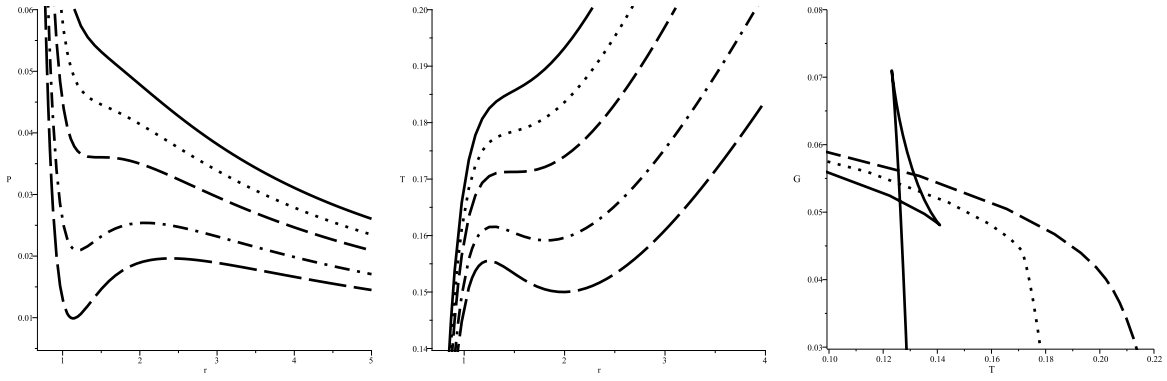


FIG. 1: "LNEF branch:"  $P-v$  (left),  $T-v$  (middle) and  $G-T$  (right) diagrams for  $q=1, \beta=1$  and  $d=5$ .  $P-v$  diagram, from up to bottom  $T=1.2T_c$ ,  $T=1.1T_c$ ,  $T=T_c$ ,  $T=0.85T_c$  and  $T=0.75T_c$ , respectively.  $T-v$  diagram, from up to bottom  $P=1.2P_c$ ,  $P=1.1P_c$ ,  $P=P_c$ ,  $P=0.85P_c$  and  $P=0.75P_c$ , respectively.  $G-T$  diagram, for  $P=0.5P_c$  (continuous line),  $P=P_c$  (dot line) and  $P=1.5P_c$  (dashed line).

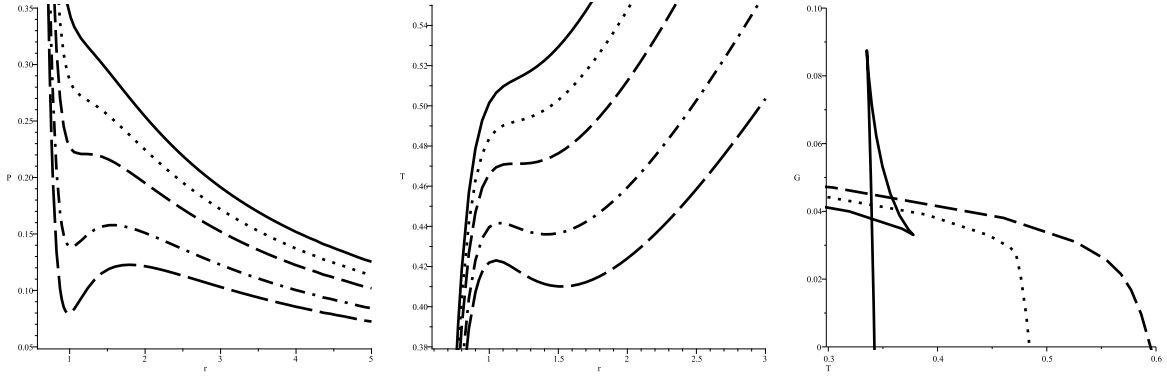


FIG. 2: "LNEF branch:"  $P-v$  (left),  $T-v$  (middle) and  $G-T$  (right) diagrams for  $q=1, \beta=1$  and  $d=7$ .  $P-v$  diagram, from up to bottom  $T=1.2T_c$ ,  $T=1.1T_c$ ,  $T=T_c$ ,  $T=0.85T_c$  and  $T=0.75T_c$ , respectively.  $T-v$  diagram, from up to bottom  $P=1.2P_c$ ,  $P=1.1P_c$ ,  $P=P_c$ ,  $P=0.85P_c$  and  $P=0.75P_c$ , respectively.  $G-T$  diagram, for  $P=0.5P_c$  (continuous line),  $P=P_c$  (dot line) and  $P=1.5P_c$  (dashed line).

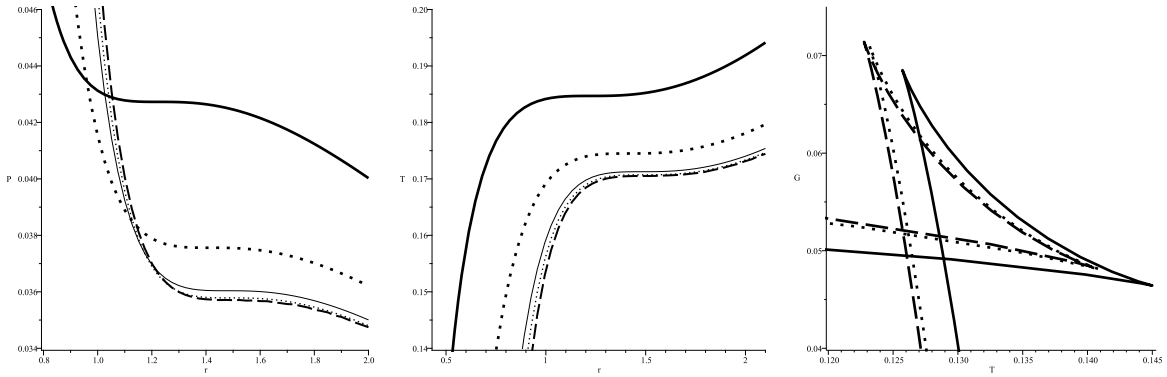


FIG. 3: "LNEF branch:"  $P-v$  (left),  $T-v$  (middle) and  $G-T$  (right) diagrams for  $q=1$  and  $d=5$ .  $P-v$  diagram, for  $T=T_c$ ,  $\beta=0.3$  (bold line),  $\beta=0.5$  (bold dot line),  $\beta=1$  (continuous line),  $\beta=1.5$ , (dot line) and  $\beta=10$  (dash line).  $T-v$  diagram, for  $P=P_c$ ,  $\beta=0.3$  (bold line),  $\beta=0.5$  (bold dot line),  $\beta=1$  (continuous line),  $\beta=1.5$ , (dot line) and  $\beta=10$  (dash line).  $G-T$  diagram, for  $P=0.5P_c$ ,  $\beta=0.5$  (continuous line),  $\beta=1$ , (dot line) and  $\beta=1.5$  (dash line).

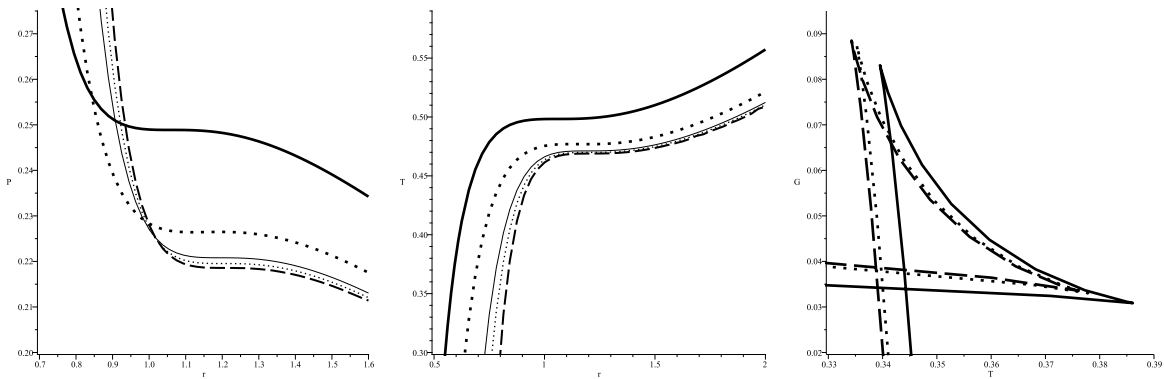


FIG. 4: "LNEF branch:"  $P - v$  (left),  $T - v$  (middle) and  $G - T$  (right) diagrams for  $q = 1$  and  $d = 7$ .

$P - v$  diagram, for  $T = T_c$ ,  $\beta = 0.3$  (bold line),  $\beta = 0.5$  (bold dot line),  $\beta = 1$  (continuous line),  $\beta = 1.5$ , (dot line) and  $\beta = 10$  (dash line).

$T - v$  diagram, for  $P = P_c$ ,  $\beta = 0.3$  (bold line),  $\beta = 0.5$  (bold dot line),  $\beta = 1$  (continuous line),  $\beta = 1.5$ , (dot line) and  $\beta = 10$  (dash line).

$G - T$  diagram, for  $P = 0.5P_c$ ,  $\beta = 0.5$  (continuous line),  $\beta = 1$ , (dot line) and  $\beta = 1.5$  (dash line).

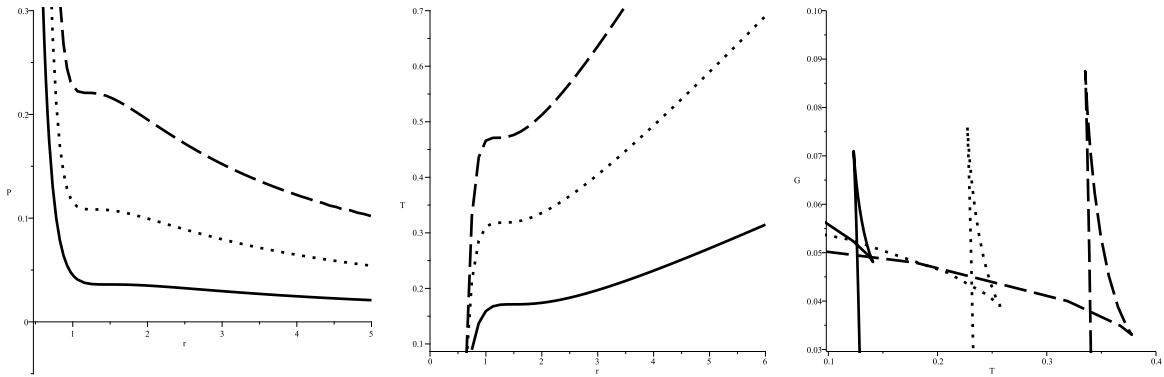


FIG. 5: "LNEF branch:"  $P - v$  (left),  $T - v$  (middle) and  $G - T$  (right) diagrams for  $q = 1$ ,  $P = 0.5P_c$  and  $\beta = 1$ .

$P - v$ ,  $T - v$  and  $G - T$  diagrams for  $d = 5$  (continuous line),  $d = 6$  (dot line) and  $d = 7$  (dashed line), respectively.

two diagrams related to two different values of nonlinearity decreases which shows the fact that the effect of nonlinearity in higher values do not change critical values so much (see the left diagrams of Figs. 3 and 4 for more details). Also, one can argue that due to fact that pressure is related to cosmological constant which is related to asymptotical curvature of the background and our thermodynamical system, as nonlinearity parameter increases, the necessity of having a background with higher curvature decreases.

As one can see in  $T - v$  diagrams, as the nonlinearity parameter increases, temperature (horizon radius) of critical points of phase transition decreases (increases) (see the middle diagram of Figs. 3 and 4). In other words, in order to have phase transition for large  $\beta$ , we need less energy which is consistent with results that we find in studying Gibbs free energy diagrams. Therefore, for having phase transition in the presence of higher value of  $\beta$ , black hole needs to absorb less mass in order to achieve stable state.

The effects of dimensionality on critical points and their behavior is another interesting issue that we discuss in this section. The obtained  $G - T$  diagram for different dimensions shows that as dimensionality increases, the temperature of critical points increases which indicates the necessity of more energy for having a phase transition (see the right diagram of Fig. 5 for more details). On the other hand, the gap between two different phases of our thermodynamical system increases which shows the fact that as dimensionality increases the change in energy of system in which phase transition occurs, increases too. For the  $P - v$  diagrams, we have higher pressure in which phase transition takes place. In other words, as dimensions of system increase pressure, hence cosmological constant increases, which is acceptable because of the fact that cosmological constant is dimension dependent (see the left diagram of Fig. 5 for more details). Finally, for the  $T - v$  diagram of Fig. 5, we can see that the temperature of critical value and the length of subcritical isobars increases which means that the single phase region of small/large black holes decreases. Therefore, as dimensionality increases the system needs to absorb more mass in order to have phase transition.

Finally, we are studying the behavior of critical values and the universal ratio of  $\frac{P_c v_c}{T_c}$ . As One can see, the critical horizon radius increases, as nonlinearity parameter increases, whereas critical temperature and pressure decrease. Also, we can see the ratio of  $\frac{P_c v_c}{T_c}$  is an increasing function of nonlinearity parameter. For higher dimensions, we have higher values of critical points which result into higher value of  $\frac{P_c v_c}{T_c}$ . Studying tables also confirms the results that we have derived through studying graphs. As the nonlinearity parameter increases, the thermodynamical system will be in need of less energy (in our black hole case by absorbing mass) in order to have phase transition.

#### IV. HEAT CAPACITY AND GTD IN EXTENDED PHASE SPACE

In this section, we expand our study regarding the critical behavior of the system in context of heat capacity and GTD. In order to study the critical behavior of the system, there are several approaches. One of these approaches is studying the behavior of the heat capacity. It is arguable that there are two types of phase transition: one is related to changes in the signature of the heat capacity. In other words, roots of the heat capacity are representing phase transitions which we will call them type one. The other type of phase transition which we will call it type two, is related to divergency of the heat capacity. It means that singularities of the heat capacity are representing places in which system goes under phase transition. For the heat capacity in extended phase space we have following relation

$$C_{Q,P} = T \left( \frac{\partial S}{\partial T} \right)_{Q,P}. \quad (20)$$

On the other hand, another approach for studying the thermodynamical behavior of the system is through thermodynamical metric. In other words, one can use a thermodynamical potential with specific set of extensive parameters in order to construct a metric. The Ricci scalar of this metric may contain divergence points in which phase transitions take place in them. It was shown that in order to this approach and heat capacity approach lead into same results, the divergencies of thermodynamical Ricci scalar (TRS) and phase transitions of the heat capacity (regardless of their type) must coincide.

The problem in constructing an effective GTD model for studying phase transitions in extended phase is the fact that  $M(S, Q, P)$  is a linear function with respect to the pressure ( $P$ ) whereas different GTD methods contain second derivation with respect to extensive parameters. Therefore, using these usual methods result into Ricci scalar of the constructed metric being zero (since  $M_{PP} = \frac{\partial^2 M}{\partial P^2} = 0$ ). To summarize, we need a model in which:

1. *All the divergence points of Ricci scalar of constructed spacetime, coincide with phase transition points of the heat capacity.*

2. *It must contain at last up to first order derivation with respect to extensive parameters (such as pressure).*

In order to making considered GTD model more effective, we will add third condition for the GTD model:

3. *The critical behavior of the Ricci scalar of the constructed spacetime must be consisting with our critical behavior that is observed in extended phase space. In other words, characteristic behavior that is observed for critical values in studying  $P-v$ ,  $T-v$  and  $G-T$  must be seen in the behavior of Ricci scalar. The critical behavior in case of  $P < P_c$ ,  $P = P_c$  and  $P > P_c$  must be consistent in all these three approaches.*

Armed with these three conditions, we will introduce the following metric for our case of study (Case I)

$$ds^2 = S \frac{M_S}{M_{QQ}^3} (-M_{SS} dS^2 + M_{QQ} dQ^2 + dP^2), \quad (21)$$

where  $M_J = \frac{\partial M}{\partial J}$  and  $M_{JJ} = \frac{\partial^2 M}{\partial J^2}$ . For economical reasons we will not bring obtained values for the heat capacity, Eq. (20), and also TRS of the constructed thermodynamical metric, Eq. (21). Since we are looking for the divergence points of TRS, it is sufficient to investigate its denominator. It is a matter of calculation to show that the denominator of TRS has the following form

$$\text{denom}(\mathcal{R}) = S^3 M_S^3 M_{SS}^2. \quad (22)$$

As one can see, the denominator of TRS contains both numerator and denominator of the heat capacity ( $M_S = T$  and  $M_{SS}$ ). Therefore, our first condition is satisfied. On the other hand, the constructed metric has more than first derivative with respect to extensive parameters and its Ricci scalar is nonzero. Therefore, our second condition is also satisfied. As for the final condition, in order to elaborate the effectiveness of this thermodynamical metric, we will plot some diagrams with respect to obtained critical values in previous sections (Figs. 6 - 9).

First of all, we should point out that there is one divergency for TRS which is related to root of the heat capacity in all plotted diagrams. As one can see, for the case of  $P = P_c$  (left and middle panels of Figs. 7 and 9), there is



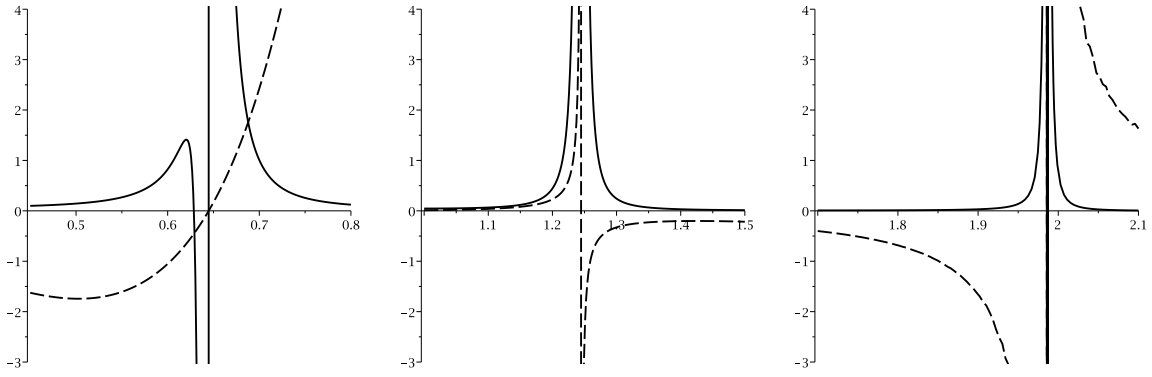


FIG. 6: "LNEF branch:"  $\mathcal{R}$  (continuous line - Case I),  $C_Q$  (dashed line) diagrams for  $d = 5$ ,  $q = 1$  and  $\beta = 1$ . for different scales:  $P = 0.75P_c$ .

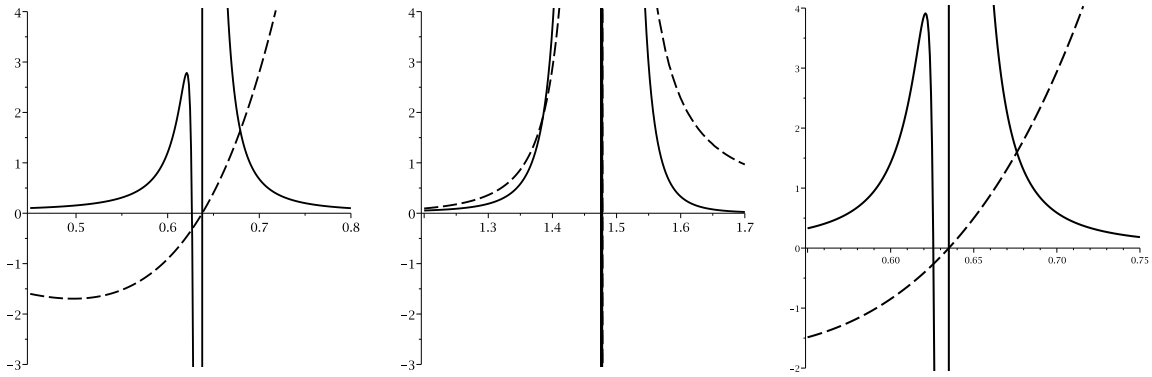


FIG. 7: "LNEF branch:"  $\mathcal{R}$  (continuous line - Case I),  $C_Q$  (dashed line) diagrams for  $d = 5$ ,  $q = 1$  and  $\beta = 1$ . for  $P = P_c$  middle and left (different scales) and  $P = 1.1P_c$  Right.

a divergency for heat capacity which is located exactly at critical horizon radius of extended phase space (compare it with table 1 and 2, and middle diagrams of Figs. 1 and 2). Also for this case, both TRS and  $C_Q$  have only one divergency at the same place. As for  $P < P_c$  (Figs. 6 and 8), there are two divergencies for the heat capacity and TRS which coincide with each other. Finally, for the case of  $P > P_c$ , no divergency is observed for the heat capacity, TRS and  $T - v$  diagrams of extended phase space (middle panels of Figs. 1 and 2, right panels of Figs. 7 and 9).

As one can see employed thermodynamical metric is providing an effective machinery in which the behaviors of

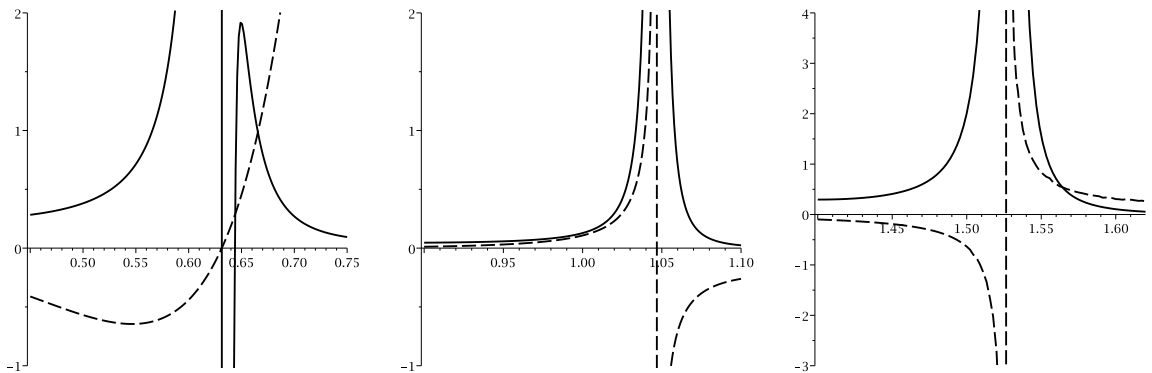


FIG. 8: "LNEF branch:"  $\mathcal{R}$  (continuous line - Case I),  $C_Q$  (dashed line) diagrams for  $d = 7$ ,  $q = 1$  and  $\beta = 1$ . for different scales:  $P = 0.75P_c$ .

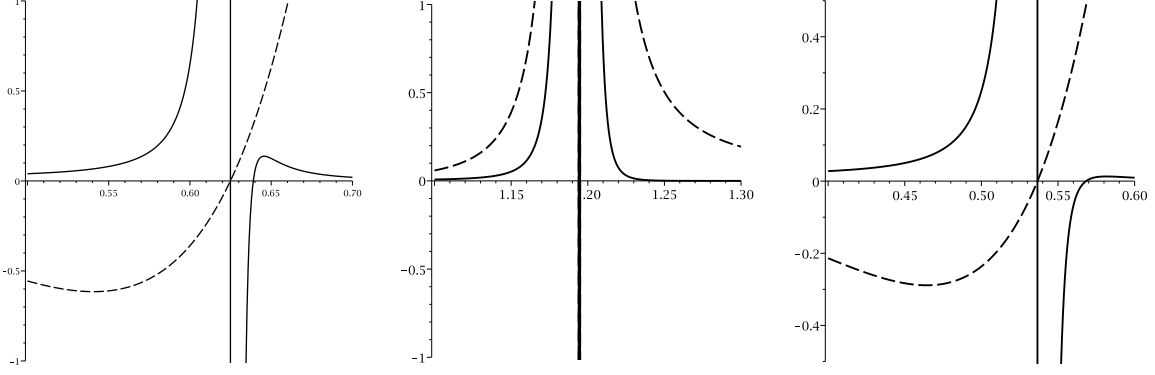


FIG. 9: "LNEF branch:"  $\mathcal{R}$  (continuous line - Case I),  $C_Q$  (dotted line) diagrams for  $d = 7$ ,  $q = 1$  and  $\beta = 1$ . for  $P = P_c$  middle and left (different scales) and  $P = 1.1P_c$  Right.

the heat capacity and phase diagrams of the extended phase space are seen. In other words, constructed spacetime posses characteristics and properties in which enable it to present all the critical behavior of the heat capacity plus extended phase space at the same time. It is worthwhile to mention that characteristic behavior of TRS enables one to both types of the phase transitions from each other. For more clarifications, we should note that for type two phase transitions, the sign of TRS remains fixed around the divergence points of the heat capacity, while in the case of type one, the sign of TRS will be changed around the root of  $C_Q$ . In addition, we should note that the critical points of the extended phase space are second order phase transitions and they match to the divergence points of the heat capacity.

Considering mentioned conditions for constructing thermodynamical metric, one can introduce another type of metric which is similar with the previous one with one difference. This metric has the following structure (Case II)

$$ds^2 = S \frac{M_S}{M_{QQ}^3} (-M_{SS}dS^2 + M_{QQ}dQ^2 + M_P dP^2), \quad (23)$$

in which, its Ricci scalar denominator will be in the following form

$$denom(\mathcal{R}) = S^3 M_S^3 M_{SS}^2 M_P^2. \quad (24)$$

As one can see, special case of existence of different orders of pressure, the  $M_P^2$  may contribute to number of the divergencies of TRS. This contribution may lead to existence of extra divergencies for the Ricci scalar which do not coincide with any phase transition point of the heat capacity. In our case (obtained solutions), due to the existence of linear function of  $P$ , there will be no contribution to number of divergencies of the heat capacity. Therefore we expect that although the total behavior of TRS may change from that of previous TRS, the places of divergencies coincides. Plotting graphs confirm that the location of divergence points of new TRS will be the same as those of previous TRS (see Figs. 10 and 11 and compare them with Figs. 6 - 9).

## V. CRITICAL VALUES THROUGH HEAT CAPACITY IN THE EXTENDED PHASE SPACE

In this section we will introduce a new method for obtaining critical pressure and horizon radius and studying the critical behavior of the system in the extended phase space. In last section it was pointed out that phase transition points in extended phase space appeared as divergence points in the heat capacity. Therefore, one can use divergencies of the heat capacity; hence root of the denominator of the heat capacity for obtaining critical values and studying critical behavior of the system. For more clarifications, we explain the method step by step.

First step is devoted to finding the heat capacity for the system under consideration. Next, we use the analogy between pressure and cosmological constant to rewrite the obtained heat capacity in the extended phase space. Then, we take into account denominator of the heat capacity and solve it with respect to pressure to obtain a relation for pressure. It should be pointed out that this relation is not same as the one that was derived for pressure in Eq. (13). In other words, these two expressions are independent of each other.

The newly obtained relation for pressure contains different information regarding critical points and the critical behavior of the system. The existence of maximum in obtained relation is representing critical pressure and horizon

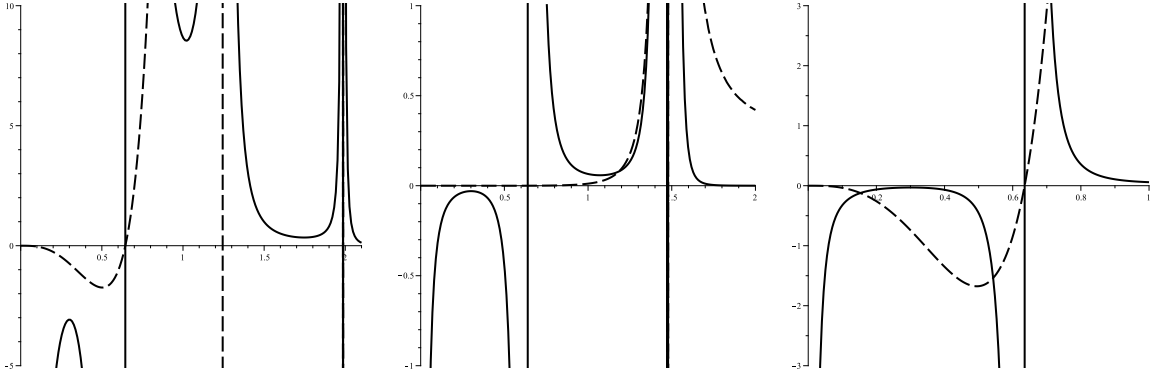


FIG. 10: "LNEF branch:"  $\mathcal{R}$  (continuous line - Case II),  $C_Q$  (dashed line) diagrams for  $d = 5$ ,  $q = 1$  and  $\beta = 1$ . for  $P = 0.75P_c$  left,  $P = P_c$  middle,  $P = 1.1P_c$  Right and .

in which phase transition takes place in it. The general behavior of the pressure in case of this relation (one or several maximum points) indicates the critical behavior of the system (one or several phase transition, triple point, regular and non-regular phase transitions). In other words, only by studying the diagrams of this relation for different values of metric function parameters one can study the critical behavior of the system. It is worthwhile to mention that absence of the maximum is representing non-critical system.

In order to elaborate the efficiency of the mentioned method, we conduct a study in case of black holes that we have been studied in this paper. As it was mentioned before, one can use Eq. (20) for obtaining heat capacity for these black holes. Using denominator of the heat capacity and solving it with respect to pressure one can find following relations for pressure for 5 and 7 dimensions

$$P = \frac{[q^2 (q^2 + 3\beta^2 r^{2d-4}) + 2\beta^4 r^{4d-8} (1 - \Gamma^3)]}{2\pi r^{2d-4} \Gamma (2\beta^2 r^{2d-4} (\Gamma - 1) + q^2 (\Gamma - 2))} \ln \left( \frac{2\beta^2 r^{2d-4} (\Gamma - 1)}{q^2} \right) + \frac{\Theta}{\mathcal{W}} \quad (25)$$

where

$$\Theta = \begin{cases} \mathcal{A}_1 + \mathcal{A}_2 + \mathcal{A}_3 & d = 5 \\ \mathcal{B}_1 + \mathcal{B}_2 + \mathcal{B}_3 & d = 7 \end{cases}, \quad (26)$$

in which  $\mathcal{A}_i$ 's and  $\mathcal{B}_i$ 's are

$$\begin{aligned} \mathcal{A}_1 &= \frac{7}{32} \Gamma^2 \beta^3 r^8 (q^2 + 2\beta^2 r^6 (1 - \Gamma)) \left[ q^4 - 2\beta^4 r^{12} - \frac{11}{2} q^2 \beta^2 r^6 \right], \\ \mathcal{A}_2 &= \frac{9\Gamma^3 \beta^3 r^8}{32} \left[ \frac{92\beta^6 r^{18} (1 - \Gamma)}{9} + \frac{4\beta^4 r^{16} (1 - \Gamma)}{3} - 21q^2 \beta^4 r^{12} \left( \Gamma - \frac{235}{189} \right) \right], \\ \mathcal{A}_3 &= \frac{9\Gamma^3 \beta^3 r^8}{32} \left[ q^6 - 2q^2 \beta^2 r^{10} \left( \Gamma - \frac{4}{3} \right) - \frac{34q^4 \beta^2 r^6 (\Gamma - \frac{241}{68})}{9} - \frac{2q^4 r^4 (\Gamma - 2)}{3} \right], \\ \mathcal{B}_1 &= \frac{11}{36} \Gamma^2 \beta^3 r^{12} (q^2 + 2\beta^2 r^{10} (1 - \Gamma)) \left[ q^4 - \frac{3}{2} \beta^4 r^{20} - \frac{27}{4} q^2 \beta^2 r^{10} \right], \\ \mathcal{B}_2 &= \frac{25\Gamma^3 \beta^3 r^{12}}{36} \left[ \frac{177\beta^6 r^{30} (1 - \Gamma)}{25} + \frac{9\beta^4 r^{28} (1 - \Gamma)}{5} - \frac{801}{50} q^2 \beta^4 r^{20} \left( \Gamma - \frac{326}{267} \right) \right], \\ \mathcal{B}_3 &= \frac{25\Gamma^3 \beta^3 r^{12}}{36} \left[ q^6 - \frac{27}{10} q^2 \beta^2 r^{18} \left( \Gamma - \frac{4}{3} \right) - \frac{86q^4 \beta^2 r^{10} (\Gamma - \frac{1073}{344})}{25} - \frac{9q^4 r^8 (\Gamma - 2)}{10} \right], \end{aligned}$$

and  $\mathcal{W} = -\frac{1}{2}\pi\Gamma^4\beta^5r^{20} [2\beta^2r^6(\Gamma - 1) + q^2(\Gamma - 2)]$ .

Next, by considering the values that are considered for different parameters in previous sections (the ones in tables 1 and 2), we plot following diagrams for 5 and 7 dimensional cases (Fig. 12).

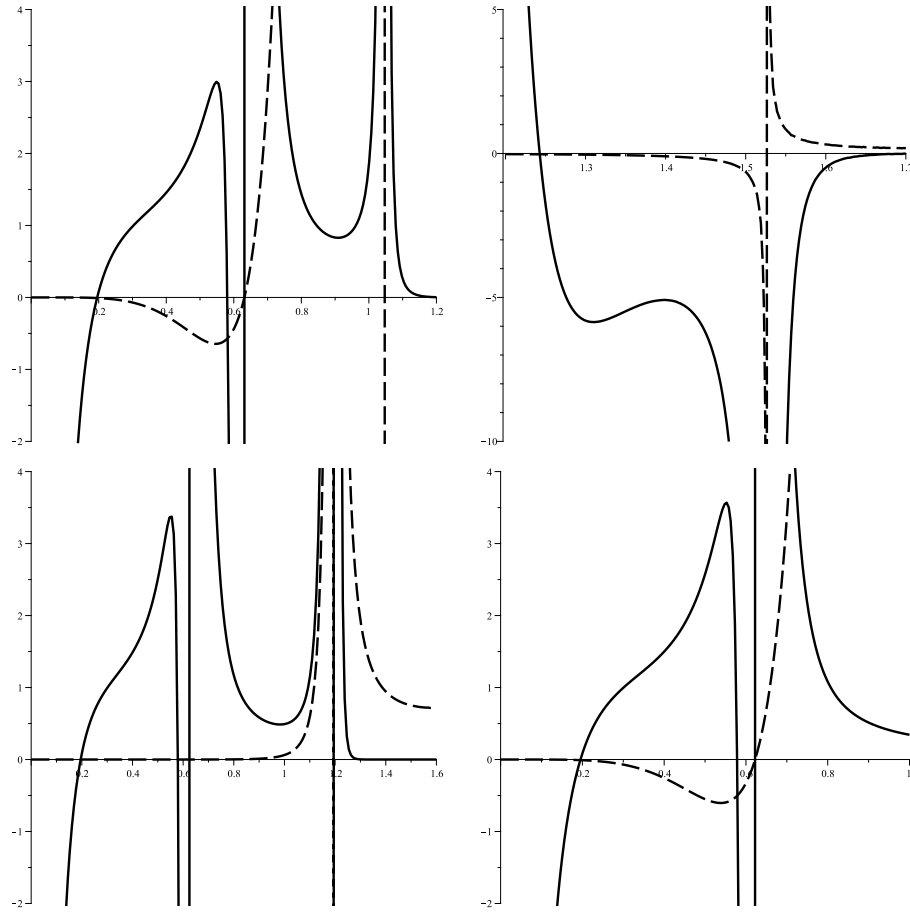


FIG. 11: "LNEF branch:"  $\mathcal{R}$  (continuous line - Case II),  $C_Q$  (dashed line) diagrams for  $d = 7$ ,  $q = 1$  and  $\beta = 1$ .  
 up:  $P = 0.75P_c$  for different scales  
 down:  $P = P_c$  left and  $P = 1.1P_c$  right

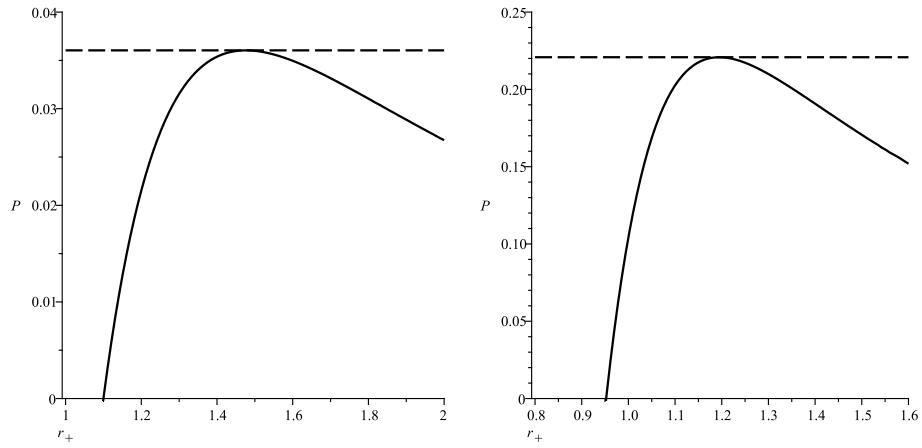


FIG. 12: "LNEF branch:"  $P$  versus  $r_{Q+}$  diagrams for  $q = 1$  and  $\beta = 1$ .  
 left panel:  $d = 5$ (continues line) and  $P = 0.0360$  (dashed line); right panel:  $d = 7$ , (continues line) and  $P = 0.2207$  (dashed line).

It is evident that for considering the mentioned values one finds that there is a maximum for plotted graphs of pressure versus horizon radius. As one can see, the pressure and horizon radius of this maximum are exactly what we have obtained in tables 1 and 2 for 5 and 7 dimensional cases. On the other hand, we see that the behavior of the pressure is exactly what we are expecting in thermodynamical aspect. There is a critical value for pressure (the maximum) in which for smaller values of the that critical pressure, there exists two critical pressure and for pressures larger than the critical pressure (maximum) there is no value for pressure, therefore, no phase transition will take place. This behavior is consistent with what we have observed in studying  $T - v$  diagrams.

There are several results regarding this study that we highlight them:

1) The thermodynamical behavior of the system, which in our case is black hole, is consistent in context of all three approaches that we have used to study the critical behavior of the system. Therefore, all of these approaches yield consisting results.

2) In order to study the thermodynamical behavior of the system, and existence of regular and non-regular critical behavior, studying the denominator of the heat capacity is sufficient. In other words, solving the denominator with respect to pressure, leads to a relation in which maximums are presenting critical values and phase transition points. Therefore, instead of using Eqs. 17 and 18, one can study the denominator of the heat capacity and its behavior.

3) Equations. 17 and 18 are usually presenting complicated set of equations which may be difficult to solve for obtaining critical values whereas studying the maximums of the obtained relation from denominator of the heat capacity for pressure is much more easier to deal with.

## VI. CONCLUSIONS

In this paper, we have considered two classes of nonlinear electrodynamics in presence of Einstein gravity and studied their phase transitions. At first, by considering cosmological constant as thermodynamical pressure and its conjugating variable as volume we have extended the phase space and regarded the interpretation of total mass of black hole as the Enthalpy. Studying calculated critical values through three different types of phase diagrams resulted into phase transition taking place in the critical values.  $P - v$ ,  $T - v$  and  $G - T$  diagrams representing similar behavior near critical points similar to their corresponding diagrams in Van der Waals liquid-gas system.

Studying the effects of nonlinearity parameter on the phase diagrams revealed the fact that as nonlinearity parameter increases the critical temperature and pressure decrease which indicates that for large values of nonlinearity parameter the system needs less energy (mass) absorption to have phase transition. Due to fact that for large  $\beta$  these nonlinear models reduce to Maxwell theory, one might conclude that the lowest temperature and pressure in which phase transition takes place, belongs to Maxwell theory. Besides, we found that the universal ratio of  $\frac{P_c v_c}{T_c}$  increases as nonlinearity parameter increases. It is worthwhile to mention that subcritical isobars in  $T - v$  are decreasing functions of nonlinearity parameter. These subcritical isobars are representing the region in which phase transition takes place which its length is a decreasing function of nonlinearity parameter.

Next, studying the effects of dimensionality showed that, for higher dimensional black holes, phase transitions take place in higher temperature and the difference between Gibbs free energy of different phases grows larger. We found that as dimensionality of black holes increases, phase transition for obtaining stable state becomes more difficult and black holes need to absorb more mass in order to have phase transition. It is worthwhile to mention the fact that dimensionality also increases the critical temperature and pressure drastically whereas it decreases the critical horizon. In other words, in comparing critical pressure and temperature of several dimensions, the highest values of these critical quantities belong to the highest dimensions.

One should take this fact into account that for small values of nonlinearity, changes in critical values are greater comparing to large values of nonlinearity parameter. This fact is evident from studying phase diagrams and tables. These differences in critical values are due to fact that as nonlinearity parameter decreases to values near zero the power of nonlinear electromagnetic fields grows stronger. This behavior indicates that as nonlinear electromagnetic field grows stronger, for having phase transition, the black hole needs to absorb more mass; hence the total mass of black hole must increase in order to have small/large (unstable/stable) black hole phase transition. In other words, in generalizing from linear theory of electrodynamics to nonlinear ones, we have fundamentally modifying the interior thermodynamical structure of the black holes. It is very important to understand the effects of the nonlinearity power. As we have seen the power of the nonlinearity decreases as the nonlinearity parameter increases which caused the critical behavior of the system be Maxwell like. Considering the mentioned nonlinear electrodynamics, we have shown not only the metric function and the electromagnetic field will be generalized, but also the critical behavior of the system will be modified in such a way that in case of large  $\beta$ , the system recover the behaviors of Reissner–Nordström black holes. On the other sides, for small values of nonlinearity parameter, the power of nonlinearity grows drastically and the critical values were highly modified. It is worthwhile to mention that for  $\beta \rightarrow 0$ , the electromagnetic field vanishes and the system switch to the Schwarzschild–like behavior which we are expecting to see no phase transition.

Taking this behavior into account, one might argue that before system attaining Schwarzschild-like behavior, it will have the highest critical temperature and pressure and the lowest critical horizon. In other words, near the Schwarzschild-like limit, critical horizon will be so small and in Schwarzschild case, the critical horizon will vanish and therefore there will be no phase transition.

Next, we employed heat capacity and GTD method in order to study the obtained critical points in extended phase space. It was pointed out that phase transition points of the extended phase space only appeared as divergencies of the heat capacity which were denoted as type two phase transitions. The characteristic behavior of heat capacity (number of divergencies of heat capacity) was similar to the one in study conducted in context of extended phase space specially  $T - v$  diagrams. On the other hand, two new geometrothermodynamical metrics were introduced for studying critical behavior of the system. In these cases, the divergencies of TRS of thermodynamical metrics coincided with phase transitions of the heat capacity. Also, the characteristic behavior of TRS for different cases of the critical values was similar to the one in extended phase space. Therefore, we established two new methods of GTD for studying critical behavior of the system in context of extended phase space.

Finally, we showed that one can use the denominator of the heat capacity for obtaining the critical pressure, horizon radius and the characteristic behavior of the system near critical point (regular and non-regular ones). In other words, solving denominator of the heat capacity with respect to pressure lead to a relation in which maximums were representing phase transition points of the system. Using the denominator of the heat capacity has certain advantages that make it more favorable in comparison with other approaches. Also, we showed that results that were found using GTD, heat capacity and extended phase space lead to consisting results. In other words, these three pictures have consisting machineries for describing critical behavior of the system.

For the future works, one may generalize obtained static solutions to a case of dynamical ones. It means that one may consider nonlinearly dynamical black hole solutions to investigate Hawking radiation. We know that the Hawking radiation decreases the total mass of black hole and according to our obtained results, one may say that this radiation shifts black hole from stable to unstable phase. In other words, Hawking radiation mechanism (black hole evaporation) affects the stability and phase transition of black holes fundamentally and makes black holes unstable in our models. It will be constructive to study a time dependent (dynamical) spacetime through Hawking radiations near the critical point.

### Acknowledgments

We thank the Shiraz University Research Council. This work has been supported financially by the Research Institute for Astronomy and Astrophysics of Maragha, Iran.

- 
- [1] J. Maldacena, *Adv. Theor. Math. Phys.* **2**, 231 (1998).
  - [2] E. Witten, *Adv. Theor. Math. Phys.* **2**, 253 (1998).
  - [3] S. S. Gubser, I. R. Klebanov, and A. M. Polyakov, *Phys. Lett. B* **428**, 105 (1998).
  - [4] O. Aharony, S. S. Gubser, J. Maldacena, H. Ooguri, and Y. Oz, *Phys. Rept.* **323**, 183 (2000).
  - [5] J. Creighton and R. B. Mann, *Phys. Rev. D* **52**, 4569 (1995).
  - [6] G. W. Gibbons, R. Kallosh, and B. Kol, *Moduli*, *Phys. Rev. Lett.* **77** 4992 (1996).
  - [7] D. Kastor, S. Ray and J. Traschen, *Class. Quantum Gravit.* **26**, 195011 (2009).
  - [8] M. Cvetič, G. W. Gibbons, D. Kubiznak and C. N. Pope, *Phys. Rev. D* **84**, 024037 (2011).
  - [9] B. P. Dolan, *Class. Quantum Gravit.* **28**, 125020 (2011).
  - [10] B. P. Dolan, *Class. Quantum Gravit.* **28**, 235017 (2011).
  - [11] D. Kubiznak and R. B. Mann, *JHEP* **07**, 033 (2012).
  - [12] S. Gunasekaran, R. B. Mann and D. Kubiznak, *JHEP* **11**, 110 (2012).
  - [13] R. Banerjee and D. Roychowdhury, *Phys. Rev. D* **85**, 104043 (2012).
  - [14] A. Lala and D. Roychowdhury, *Phys. Rev. D* **86**, 084027 (2012).
  - [15] R. Banerjee and D. Roychowdhury, *Phys. Rev. D* **85**, 044040 (2012).
  - [16] S. H. Hendi and M. H. Vahidinia, *Phys. Rev. D* **88**, 084045 (2013).
  - [17] D. C. Zou, S. J. Zhang and B. Wang, *Phys. Rev. D* **89**, 044002 (2014).
  - [18] S. W. Hawking and D. N. Page, *Commun. Math. Phys.* **87**, 577 (1983).
  - [19] E. Witten, *Adv. Theor. Math. Phys.* **2**, 505 (1998).
  - [20] D. H. Delphenich, [arXiv:0309108].
  - [21] D. H. Delphenich, [arXiv:0610088].
  - [22] M. Hassaine and C. Martinez, *Phys. Rev. D* **75**, 027502 (2007).
  - [23] S. H. Hendi and H. R. Rastegar-Sedeqi, *Gen. Relativ. Gravit.* **41**, 1355 (2009).

- [24] S. H. Hendi, Phys. Lett. B **677**, 123 (2009).
- [25] H. Maeda, M. Hassaine and C. Martinez, Phys. Rev. D **79**, 044012 (2009).
- [26] S. H. Hendi and B. Eslam Panah, Phys. Lett. B **684**, 77 (2010).
- [27] S. H. Hendi, Eur. Phys. J. C **69**, 281 (2010).
- [28] H. P. de Oliveira, Class. Quantum Gravit. **11**, 1469 (1994).
- [29] B. L. Altshuler, Class. Quantum Gravit. **7**, 189 (1990).
- [30] H. H. Soleng, Phys. Rev. D **52**, 6178 (1995).
- [31] S. H. Hendi, JHEP **03**, 065 (2012).
- [32] N. Seiberg and E. Witten, JHEP **09**, 032 (1999).
- [33] M. Born and L. Infeld, Proc. R. Soc. A **144**, 425 (1934).
- [34] E. Fradkin and A. Tseytlin, Phys. Lett. B **163**, 123 (1985).
- [35] R. Matsuavaev, M. Rahmanov and A. Tseytlin, Phys. Lett. B **193**, 207 (1987).
- [36] E. Bergshoeff, E. Sezgin, C. Pope and P. Townsend, Phys. Lett. B **188**, 70 (1987).
- [37] C. Callan, C. Lovelace, C. Nappi and S. Yost, Nucl. Phys. B **308**, 221 (1988).
- [38] O. Andreev and A. Tseytlin, Nucl. Phys. B **311**, 221 (1988).
- [39] R. Leigh, Mod. Phys. Lett. A **04**, 2767 (1989).
- [40] F. Weinhold, J. Chem. Phys. **63**, 2479 (1975).
- [41] G. Ruppeiner, Phys. Rev. A **20**, 1608 (1979).
- [42] H. Janyszek, Rep. Math. Phys. **24**, 1 (1986).
- [43] E. J. Brody, Phys. Rev. Lett. **58**, 179 (1987).
- [44] B. P. Dolan, D. A. Johnston and R. Kenna, J. Phys. A **35**, 9025 (2002).
- [45] W. Janke, D. A. Johnston and R. Kenna, Physica A **336**, 181 (2004).
- [46] S. Ferrara, G. W. Gibbons and R. Kallosh, Nucl. Phys. B **500**, 75 (1997).
- [47] R. G. Cai and J. H. Cho, Phys. Rev. D **60**, 067502 (1999).
- [48] J. E. Aman, I. Bengtsson and N. Pidokrajt, Gen. Relativ. Gravit. **35**, 1733 (2003) .
- [49] S. Carlip and S. Vaidya, Class. Quantum Gravit. **20**, 3827 (2003).
- [50] B. Mirza and M. Zamani-Nasab, JHEP **06**, 059 (2007) .
- [51] S. H. Hendi, S. Panahiyan, B. Eslam Panah and M. Momennia, *A new approach toward geometrical concept of black hole thermodynamics*, submitted for publication.
- [52] H. Quevedo, J. Math. Phys. **48**, 013506 (2007).
- [53] H. Quevedo and A. Sanchez, JHEP **09**, 034 (2008).
- [54] J. X. Mo, X. X. Zeng, G. Q. Li, X. Jiang and W. B. Liu, JHEP **10**, 056 (2013).
- [55] J. L. Zhang, R. G. Cai and H. Yu, JHEP **02**, 143 (2015).
- [56] H. Quevedo, A. Sanchez, S. Taj and A. Vazquez, Gen. Relativ. Gravit. **43**, 1153 (2011).
- [57] Y. Han, G. Chen, Phys. Lett. B **714**, 127 (2012).
- [58] A. Bravetti, D. Momeni, R. Myrzakulov and A. Altaibayeva, Adv. High Energy Phys. **2013**, 549808 (2013).
- [59] S. H. Hendi, Ann. Phys. **346**, 42 (2014).
- [60] S. H. Hendi, Ann. Phys. **333**, 282 (2013).
- [61] S. H. Hendi and M. Allahverdizadeh, Adv. High Energy Phys. 390101 (2014).
- [62] S. H. Hendi and A. Sheykhi, Phys. Rev. D **88**, 044044 (2014).
- [63] L. Brewin, Gen. Relativ. Gravit. **39**, 521 (2007).
- [64] D. Kastor, S. Ray and J. Traschen, Class. Quant. Grav. **27**, 235014 (2010).
- [65] R. G. Cai, L. M. Cao, L. Li and R.Q. Yang, JHEP **09**, 005 (2013).
- [66] D. C. Zou, S. J. Zhang and B. Wang, Phys. Rev. D **89**, 044002 (2014).
- [67] Z. Sherkatghanad, B. Mirza, Z. Mirzaeyan and S. A. H. Mansoori, [arXiv:1412.5028].